ChemPubSoc Europe

DOI: 10.1002/cphc.201500011

CHEMPHYSCHEM Communications

# Intense Upconversion Luminescence of $CaSc_2O_4$:$Ho^{3+}$/$Yb^{3+}$ from Large Absorption Cross Section and Energy-Transfer Rate of $Yb^{3+}$

Jing Li,[a, b] Jiahua Zhang,*[a] Zhendong Hao,[a] Li Chen,[b] Xia Zhang,[a] and Yongshi Luo[a]

Concentration-optimized $CaSc_2O_4$:0.2%$Ho^{3+}$/10%$Yb^{3+}$ shows stronger upconversion luminescence (UCL) than a typical concentration-optimized upconverting phosphor $Y_2O_3$:0.2%$Ho^{3+}$/10%$Yb^{3+}$ upon excitation with a 980 nm laser diode pump. The $^5F_4+{}^5S_2\rightarrow{}^5I_8$ green UCL around 545 nm and $^5F_5\rightarrow{}^5I_8$ red UCL around 660 nm of $Ho^{3+}$ are enhanced by factors of 2.6 and 1.6, respectively. On analyzing the emission spectra and decay curves of $Yb^{3+}$: $^2F_{5/2}\rightarrow{}^2F_{7/2}$ and $Ho^{3+}$: $^5I_6\rightarrow{}^5I_8$, respectively, in the two hosts, we reveal that $Yb^{3+}$ in $CaSc_2O_4$ exhibits a larger absorption cross section at 980 nm and subsequent larger $Yb^{3+}$: $^2F_{5/2}\rightarrow Ho^{3+}$: $^5I_6$ energy-transfer coefficient ($8.55\times10^{-17}$ $cm^3s^{-1}$) compared to that ($4.63\times10^{-17}$ $cm^3s^{-1}$) in $Y_2O_3$, indicating that $CaSc_2O_4$:$Ho^{3+}$/$Yb^{3+}$ is an excellent oxide upconverting material for achieving intense UCL.

Owing to its intense green emission under excitation at 455 nm, which is comparable to the commercial yttrium aluminum garnet (YAG):$Ce^{3+}$ phosphor, $Ce^{3+}$-doped $CaSc_2O_4$ is considered as one of the most efficient downconversion photoluminescence materials.[1] Infrared-to-visible upconversion luminescence (UCL) has been extensively studied in various oxide hosts for its potential applications in the detection of infrared light, display technologies, and biological medicine.[2–5] The $CaSc_2O_4$ oxide host lattice has a low cutoff phonon frequency of only 540 $cm^{-1}$, which can better inhibit non-radiative multiphonon relaxations in the UCL process, achieving highly efficient luminescence.[6] Limited work has been carried out on the UCL of rare-earth-metal-doped $CaSc_2O_4$ materials. Our group has reported the intense UCL in $Tm^{3+}$/$Yb^{3+}$ co-doped $CaSc_2O_4$.[6] The near-infrared emission around 800 nm of $Tm^{3+}$ is enhanced by 3.5 times, compared with that in the typical oxide host $Y_2O_3$. $Ho^{3+}$ is one of the most important active ions, owing to its intense green UCL.[7] But, fewer studies on the UCL of $Ho^{3+}$-doped materials have been reported in contrast with $Tm^{3+}$ ions. By combining the promising optical properties of $Ho^{3+}$ and good qualities of $CaSc_2O_4$, the UCL properties of $Ho^{3+}$ in the $CaSc_2O_4$ host deserve special attention.

[a] Prof. J. Li, J. Zhang, Z. Hao, X. Zhang, Y. Luo
State Key Laboratory of Luminescence and Applications
Changchun Institute of Optics, Fine Mechanics and Physics
Chinese Academy of Sciences
3888 Eastern South Lake Road, Changchun 130033 (China)
E-mail: zhangjh@ciomp.ac.cn

[b] Prof. J. Li, L. Chen
ChangChun University of Technology
A1018 Huguang Road, Changchun 130012 (China)

In this Communication, we report a large enhancement of UCL in concentration-optimized $CaSc_2O_4$:0.2%$Ho^{3+}$/10%$Yb^{3+}$. UCL intensities around 545 and 660 nm are enhanced by factors of 2.6 and 1.6, respectively, in comparison with that of concentration-optimized $Y_2O_3$:0.2%$Ho^{3+}$/10%$Yb^{3+}$. The UCL enhancement is attributed to the larger absorption cross section at 980 nm of $Yb^{3+}$ and subsequent larger $Yb^{3+}\rightarrow Ho^{3+}$ energy-transfer coefficient in $CaSc_2O_4$ than in $Y_2O_3$.

A large number experiments show that $CaSc_2O_4$:$Ho^{3+}$/$Yb^{3+}$ exhibits stronger UCL than $Y_2O_3$:$Ho^{3+}$/$Yb^{3+}$. Figure 1 shows

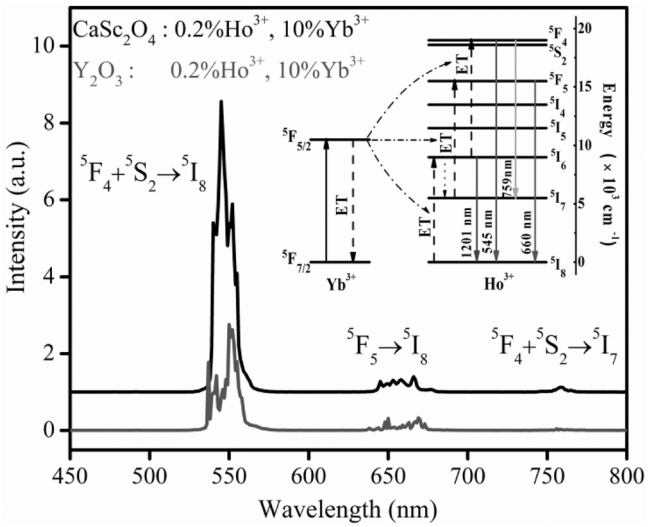


**Figure 1.** UCL spectra of concentration-optimized $CaSc_2O_4$:0.2%$Ho^{3+}$/10%$Yb^{3+}$ and $Y_2O_3$:0.2%$Ho^{3+}$/10%$Yb^{3+}$ under 980 nm excitation with a low pump density (7 mW $mm^{-2}$). Inset shows the energy-level diagrams and energy-transfer pathways.

the UCL spectra of concentration-optimized $CaSc_2O_4$:0.2%$Ho^{3+}$/10%$Yb^{3+}$ and $Y_2O_3$:0.2%$Ho^{3+}$/10%$Yb^{3+}$ under 980 nm excitation with an output power density of 7 mW $mm^{-2}$. The spectra exhibit three UC emissions peaked around 545, 660, and 759 nm, which are assigned to the $^5F_4+{}^5S_2\rightarrow{}^5I_8$, $^5F_5\rightarrow{}^5I_8$, and $^5F_4+{}^5S_2\rightarrow{}^5I_7$ transitions of $Ho^{3+}$, respectively.[10] The pathways for UC emissions are demonstrated schematically under 980 nm excitation in the inset of Figure 1. Compared with $Y_2O_3$:$Ho^{3+}$/$Yb^{3+}$, stronger UCL is observed in $CaSc_2O_4$:$Ho^{3+}$/$Yb^{3+}$. The green (545 nm) and red (660 nm) UCL intensities are enhanced by a remarkable factor of 2.6 and 1.6 in $CaSc_2O_4$, respectively.

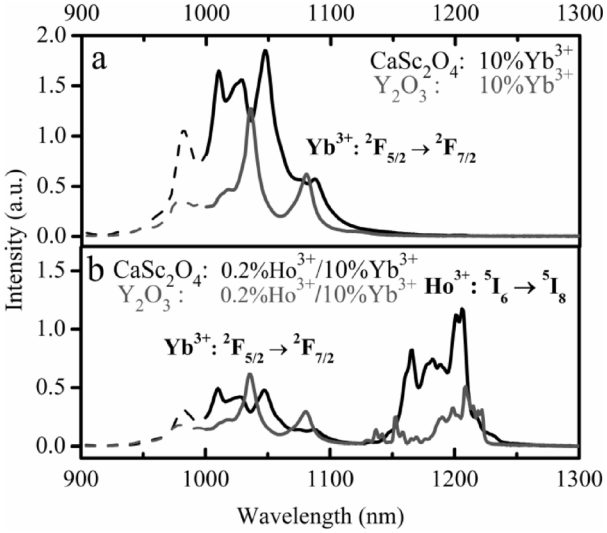


**Figure 2.** Infrared emission spectra of a) 10% $Yb^{3+}$ singly doped and b) 0.2% $Ho^{3+}$/10% $Yb^{3+}$ co-doped $CaSc_2O_4$ and $Y_2O_3$ under 980 nm excitation with the same pump density (7 mW mm$^{-2}$).

To understand the UCL enhancement, we focus on a comparison of the absorption capacities at 980 nm by $Yb^{3+}$ in the two hosts and the energy-transfer rates from $Yb^{3+}$ to $Ho^{3+}$. Figure 2a shows emission spectra of $Yb^{3+}$ singly doped $CaSc_2O_4$:10% $Yb^{3+}$ and $Y_2O_3$:10% $Yb^{3+}$ upon 980 nm excitation with an output power density of 7 mW mm$^{-2}$. The spectra show typical $^2F_{5/2} \rightarrow {}^2F_{7/2}$ emissions of $Yb^{3+}$. The area emission intensity ($I_1$) of $Yb^{3+}$ in $CaSc_2O_4$ is about 2.4 times that in $Y_2O_3$. As $Ho^{3+}$/$Yb^{3+}$ is co-doped in the two hosts, $Ho^{3+}$:$^5I_6 \rightarrow {}^5I_8$ emissions around 1200 nm are found, and the area intensity ($I_2$) of which in $CaSc_2O_4$ is 2.9 times stronger than that in $Y_2O_3$, as shown in Figure 2b. Meanwhile, the emission of $Yb^{3+}$ in $CaSc_2O_4$ has a faster reduction. The results indicate that $Yb^{3+}$ absorptivity is larger at a pump wavelength of 980 nm and $Yb^{3+} \rightarrow Ho^{3+}$ energy transfer is more efficient in $CaSc_2O_4$ than that in $Y_2O_3$.

Figure 3a shows the decay curves of $Yb^{3+}$:$^2F_{5/2} \rightarrow {}^2F_{7/2}$ emission under pulsed 980 nm excitation in the $Yb^{3+}$ singly doped and $Ho^{3+}$/$Yb^{3+}$ co-doped $CaSc_2O_4$ and $Y_2O_3$ samples. As $Ho^{3+}$ is co-doped, the decays rapidly speed up, reflecting remarkable $Yb^{3+} \rightarrow Ho^{3+}$ energy transfer. The $Yb^{3+}$:$^2F_{5/2}$ lifetimes ($\tau_1$) for 10% $Yb^{3+}$ singly ($\tau_{11}$) and 0.2% $Ho^{3+}$/10% $Yb^{3+}$ doubly ($\tau_{12}$) doped samples are calculated by integrating the area under the corresponding decay curves with the normalized initial intensity, as listed in Table 1. The intrinsic lifetimes ($\tau_{10}$) are taken from our previous studies in dilute $Yb^{3+}$-doped samples.[6] The emission efficiency ($\eta_1$) can be calculated by $\eta_1 = \tau_1/\tau_{10}$. The $Yb^{3+} \rightarrow Ho^{3+}$ energy-transfer efficiency ($\eta_{ET}$) can be calculated by $\eta_{ET} = 1 - \tau_{12}/\tau_{11}$. Hence, the quenching efficiency ($\eta_q$) is deduced by $1 - \eta_1 - \eta_{ET}$.

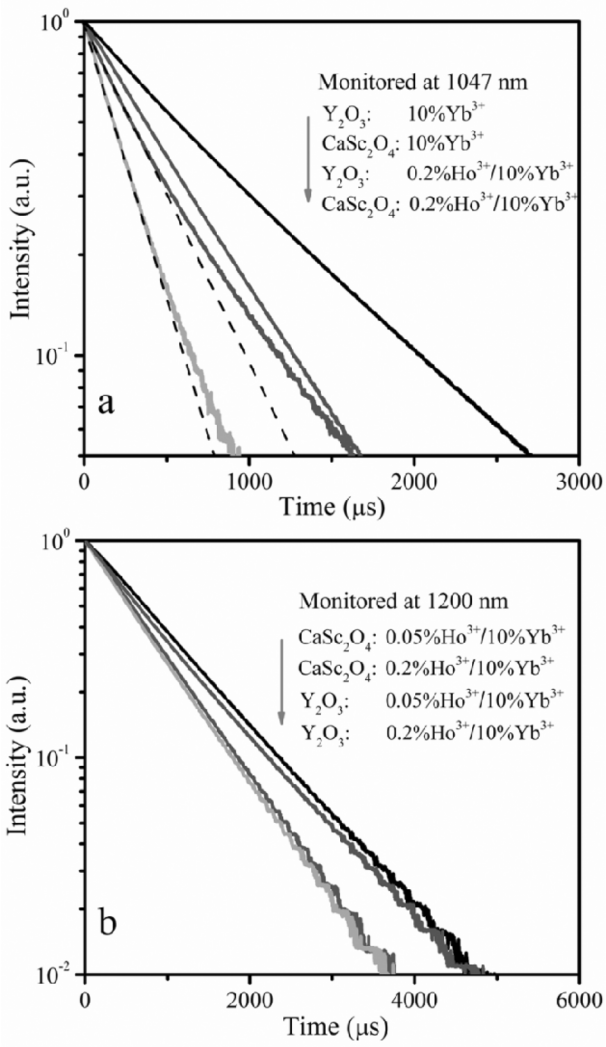


**Figure 3.** Decay curves of a) $Yb^{3+}$:$^2F_{5/2} \rightarrow {}^2F_{7/2}$ emission at 1047 nm and b) $Ho^{3+}$:$^5I_6 \rightarrow {}^5I_8$ emission at 1200 nm for doped $CaSc_2O_4$ and $Y_2O_3$ under pulsed 980 nm excitation.

Figure 3b shows the decay curves of the $Ho^{3+}$:$^5I_6 \rightarrow {}^5I_8$ emission for the 0.05% $Ho^{3+}$ or 0.2% $Ho^{3+}$ with 10% $Yb^{3+}$ doubly

**Table 1.** Intensities and lifetimes of $Yb^{3+}$:$^2F_{5/2} \rightarrow {}^2F_{7/2}$ emissions as well as the parameters for $Yb^{3+}$ absorption and $Yb^{3+} \rightarrow Ho^{3+}$ energy transfer in $CaSc_2O_4$ and $Y_2O_3$.

| Sample | $I_1$ | $\tau_1$ [μs] | $\eta_1$ | $\eta_q$ | $\eta_{ET}$ | $A$ | $\sigma$ | $C$ [cm$^3$ s$^{-1}$] | $x_C$ [cm$^{-3}$] |
|---|---|---|---|---|---|---|---|---|---|
| $CaSc_2O_4$:0.2% $Yb^{3+}$ [4] | | $\tau_{10}$: 671 | 1 | 0 | 0 | | | | |
| $CaSc_2O_4$:10% $Yb^{3+}$ | 2.4$\theta_1$ | $\tau_{11}$: 548 | 0.81 | 0.19 | 0 | 2.7 | 2.9 | | |
| $CaSc_2O_4$:0.2% $Ho^{3+}$/10% $Yb^{3+}$ | | $\tau_{12}$: 286 | 0.43 | 0.09 | 0.48 | 2.6 | 2.8 | $8.55 \times 10^{-17}$ | $1.74 \times 10^{19}$ |
| $Y_2O_3$:0.2% $Yb^{3+}$ [4] | | $\tau_{10}$: 932 | 1 | 0 | 0 | | | | |
| $Y_2O_3$:10% $Yb^{3+}$ | $\theta_1$ | $\tau_{11}$: 835 | 0.90 | 0.10 | 0 | 1 | 1 | | |
| $Y_2O_3$:0.2% $Ho^{3+}$/10% $Yb^{3+}$ | | $\tau_{12}$: 479 | 0.51 | 0.07 | 0.42 | 1 | 1 | $4.63 \times 10^{-17}$ | $2.32 \times 10^{19}$ |

doped $CaSc_2O_4$ and $Y_2O_3$ samples under pulsed 980 nm excitation. $Ho^{3+}$:$^5I_6$ exhibits a single exponential decay, indicating no back energy-transfer from $Ho^{3+}$ to $Yb^{3+}$. The decay for $CaSc_2O_4$ is much slower than that observed in the $Y_2O_3$ host. The long-lived intermediate state, $^5I_6$, is the basis of intense green UCL.[10] The average lifetimes ($\tau_2$) and emission efficiencies ($\eta_2$) of the $Ho^{3+}$:$^5I_6$ level obtained from these decay patterns are listed in Table 2. It is found that the $\tau_2$ gets slightly shorter when increasing the $Ho^{3+}$ concentration from 0.05 to 0.2%, indicating a weak quenching. The $\eta_2$ value is close to 1.

**Table 2.** Intensities and lifetimes of $Ho^{3+}$ emissions in $CaSc_2O_4$ and $Y_2O_3$.

| Sample | $I_2$ | $\tau_2$ [μs] | $\eta_2$ | $I_3$ | $\tau_3$ [μs] | $I_4$ | $\tau_4$ [μs] |
|---|---|---|---|---|---|---|---|
| $CaSc_2O_4$:0.05%$Ho^{3+}$,10%$Yb^{3+}$ | | 1039 | 1 | | | | |
| $CaSc_2O_4$:0.2%$Ho^{3+}$,10%$Yb^{3+}$ | $2.9\theta_2$ | 960 | 0.92 | $1.6\theta_3$ | 410 | $2.6\theta_4$ | 249 |
| $Y_2O_3$: 0.05%$Ho^{3+}$,10%$Yb^{3+}$ | | 812 | 1 | | | | |
| $Y_2O_3$: 0.2%$Ho^{3+}$,10%$Yb^{3+}$ | $\theta_2$ | 774 | 0.95 | $\theta_3$ | 395 | $\theta_4$ | 224 |

For $Yb^{3+}$ singly doped samples, the absorptivity ($A$) of $Yb^{3+}$ at 980 nm can be estimated by $I_1 = PA\eta_1$, where $P$ is the pump density. The absorptivity of $Yb^{3+}$ in $CaSc_2O_4$:10%$Yb^{3+}$ is 2.7 times bigger than that in $Y_2O_3$:10%$Yb^{3+}$. When $Ho^{3+}$ is co-doped, the efficient $Yb^{3+}\rightarrow Ho^{3+}$ energy transfer is observed. Owing to the fact that $Ho^{3+}$ ions are almost in the ground state under weak excitation in this work, the calculated transfer efficiency ($\eta_{ET}$) is dominantly responsible for the energy transfer to excite $Ho^{3+}$ from its ground state, $^5I_8$, to $^5I_6$. So, the absorptivity of $Yb^{3+}$ in the $Ho^{3+}$/$Yb^{3+}$ doubly doped samples can be estimated by using $\eta_{ET}$, the measured emission intensity ($I_2$), and the efficiency ($\eta_2$) of $Ho^{3+}$:$^5I_6$, which satisfy the relationship $I_2 = PA\eta_{ET}\eta_2$. The ratio of absorptivity in $CaSc_2O_4$ to that in $Y_2O_3$ is calculated to be 2.6 for the 0.2%$Ho^{3+}$/10%$Yb^{3+}$ doubly doped samples. The two values of $A$ ratios are consistent before and after energy transfer, showing the validity of the obtained $A$ values. The ratio of absorption cross section ($\sigma$) of $Yb^{3+}$ at 980 nm in $CaSc_2O_4$ to that in $Y_2O_3$ is calculated to be 2.9 for singly doped 10%$Yb^{3+}$ and 2.8 for 0.2%$Ho^{3+}$/10%$Yb^{3+}$ doubly doped samples, using the value of $A/N$, where $N$ is the $Yb^{3+}$ number per volume, $1.2\times10^{21}$ $cm^{-3}$ in $CaSc_2O_4$ and $1.3\times10^{21}$ $cm^{-3}$ in $Y_2O_3$.

It can be also seen in Figure 3a that the initial decay rate of $Yb^{3+}\rightarrow Ho^{3+}$ energy transfer lasts longer in $CaSc_2O_4$ than $Y_2O_3$, which is beneficial for highly effective energy transfer. The initial energy transfer rate, $W_{ETi}$, could be calculated by $W_{12i}-1/\tau_{11}$, where $W_{12i}$ is the initial decay rate for the doubly doped samples. The $Yb^{3+}\rightarrow Ho^{3+}$ energy-transfer coefficient ($C$) at $t=0$ can be expressed as $W_{ETi} = Cx$, where $x$ is the $Ho^{3+}$ concentration, which was $2.4\times10^{19}$ $cm^{-3}$ in $CaSc_2O_4$ and $2.6\times10^{19}$ $cm^{-3}$ in $Y_2O_3$, in this work.[11] Then, we obtained a transfer coefficient of $8.55\times10^{-17}$ $cm^3s^{-1}$ for $CaSc_2O_4$:0.2%$Ho^{3+}$/10%$Yb^{3+}$ and $4.63\times10^{-17}$ $cm^3s^{-1}$ for $Y_2O_3$:0.2%$Ho^{3+}$/10%$Yb^{3+}$. The former transfer coefficient was twice as large as the latter. The corresponding critical $Ho^{3+}$ concentration $x_c$ values, defined as $Cx_c = 1/\tau_{10}$, were determined to be $1.74\times10^{19}$ and $2.32\times10^{19}$ $cm^{-3}$, respectively.

The lifetimes associated with the red ($\tau_3$) and green ($\tau_4$) emissions in 0.2%$Ho^{3+}$/10%$Yb^{3+}$ co-doped samples are also listed in Table 2 under pulsed 980 nm excitation. The values of $\tau_3$ and $\tau_4$ are both longer in $CaSc_2O_4$ than in $Y_2O_3$. The lifetime of an energy level is proportional to the population.[10] It also indicates stronger red and green UCL in $CaSc_2O_4$:0.2%$Ho^{3+}$/10%$Yb^{3+}$.

The $CaSc_2O_4$ lattice, which owns an orthorhombic $CaFe_2O_4$ structure with the space group *Pnam* (62) exhibits a lower crystal-field symmetry than cubic $Y_2O_3$. Low-symmetry hosts exert a crystal field containing more uneven components around the dopant ions, which can improve the transition probabilities.[12] The $Yb^{3+}\rightarrow Ho^{3+}$ energy-transfer efficiency in $CaSc_2O_4$:0.2%$Ho^{3+}$/10%$Yb^{3+}$ is larger than that in $Y_2O_3$:0.2%$Ho^{3+}$/10%$Yb^{3+}$, as shown in Table 1. This can be attributed to the fact that the ground-state splitting of $Yb^{3+}$ (1008 $cm^{-1}$) in $CaSc_2O_4$ is larger than that (931 $cm^{-1}$) in $Y_2O_3$, owing to the fact that $Yb^{3+}$ on the $Sc^{3+}$ site in $CaSc_2O_4$ experiences a stronger crystal field than $Yb^{3+}$ on the $Y^{3+}$ site in $Y_2O_3$, and the mean distance between the nearest two Sc atoms (Sc–Sc) in $CaSc_2O_4$ is 3.186 Å, which is much shorter than the Y–Y distance (3.752 Å) in $Y_2O_3$.[6] Considering the equipment exists, the response time to the 980 nm laser, which is around 73 μs (according to our lifetime measurement), and fast initial decays caused by energy transfer of the nearest neighbor ions cannot been observed (≈ns);[3,13] the real lifetime value was lower than the experimental one in our study. Reabsorption effects also cause significant lengthening of the measured fluorescence lifetimes.[14] The real $\eta_{ET}$ values were larger than the experimental data. But, the relative ratio of $\eta_{ET}$ in the two hosts was less affected by it, which could be used for our above physical analysis.[14]

Compared with energy-transfer efficiency, the larger absorption cross section at 980 nm of $Yb^{3+}$ (three times that in $Y_2O_3$) plays an important role in the achievement of the strong $Ho^{3+}$:$^5I_6\rightarrow{}^5I_8$ emission in the $CaSc_2O_4$ sample. As a result, the 2.6-fold enhanced green and 1.6-fold enhanced red emissions were observed in $CaSc_2O_4$:0.2%$Ho^{3+}$/10%$Yb^{3+}$. The green emission inherits the enhanced emission from $Ho^{3+}$:$^5I_6$. The acquired enlarged values of intensities are comparable. The smaller increase in the red UCL is perhaps a result of the weak multiphonon relaxation from $^5I_6$ to $^5I_7$ in $CaSc_2O_4$. The energy gap between the $^5I_6$ and $^5I_7$ levels is around 3240 $cm^{-1}$.[15] The $CaSc_2O_4$ oxide host has a lower cutoff phonon frequency of 540 $cm^{-1}$ compared to $Y_2O_3$ (600 $cm^{-1}$), which suppresses non-radiative relaxation. This explanation requires evidence, which will be obtained by further study in the future.

In summary, we observed a largely enhanced UCL in $CaSc_2O_4$:0.2%$Ho^{3+}$/10%$Yb^{3+}$ upon excitation with a 980 nm laser diode pump. Compared with concentration-optimized $Y_2O_3$:0.2%$Ho^{3+}$/10%$Yb^{3+}$, the green and red UCL were enhanced by a factor of 2.6 and 1.6, respectively. The larger absorption cross section at 980 nm for $Yb^{3+}$ (three times that of

$Y_2O_3$) and the $Yb^{3+}$:$^2F_{5/2}$→$Ho^{3+}$:$^5I_6$ energy-transfer coefficient (twice that of $Y_2O_3$) play important roles for the achievement of intense UCL in the $CaSc_2O_4$ phosphor. $CaSc_2O_4$:$Ho^{3+}$/$Yb^{3+}$ is a promising upconverting oxide material for achieving highly efficient green UCL with diverse applications.

## Experimental Section

The doped $CaSc_2O_4$ powder samples were synthesized by using a common solid-state reaction at 1500 °C for 4 h.[8] $Y_2O_3$ samples for comparison with $CaSc_2O_4$ were prepared through the reported sol–gel method.[9] Our experiments showed that the sol–gel method for the preparation of $Y_2O_3$ is more favorable for the achievement of high crystallinity, uniform distribution of active ions ($Yb^{3+}$ and $Ho^{3+}$), and intense UCL than the solid-state reaction. Both of the produced $CaSc_2O_4$ and $Y_2O_3$ samples had a high crystallinity. The $CaSc_2O_4$:0.2%$Ho^{3+}$/10%$Yb^{3+}$ and $Y_2O_3$:0.2%$Ho^{3+}$/10%$Yb^{3+}$ samples were optimized for the highest green UCL intensity in each host.[9,10] The $Ho^{3+}$ and $Yb^{3+}$ ions occupied $Sc^{3+}$ sites in $CaSc_2O_4$ or $Y^{3+}$ sites in $Y_2O_3$. The UCL spectra were measured by using a Triax 550 spectrometer (Jobin–Yvon) pumped with a power-controllable 980 nm diode laser. In fluorescence-lifetime measurements, a pulsed 980 nm laser of an optical parametric oscillator (OPO) was used as an excitation source, and the signals were detected by a Tektronix digital oscilloscope (TDS 3052).

## *Acknowledgements*

*This work is supported by the National Natural Science Foundation of China (10834006, 51172226, 61275055, 11274007, 11174278) and the Natural Science Foundation of Jilin province (201205024).*

**Keywords:** dynamics · energy transfer · $Ho^{3+}$/$Yb^{3+}$ · luminescence · phosphors

[1] Y. Shimomura, T. Kurushima, N. Kijima, *J. Electrochem. Soc.* **2007**, *154*, J234 – J238.
[2] M. Nyk, R. Kumar, T. Y. Ohulchanskyy, E. J. Bergey, P. N. Prasad, *Nano Lett.* **2008**, *8*, 3834 – 3838.
[3] J. H. Zhang, Z. D. Hao, J. Li, X. Zhang, Y. S. Luo, G. H. Pan, *Light Sci. Appl.* **2015**, *4*, e239.
[4] M. K. Tsang, G. X. Bai, J. H. Hao, *Chem. Soc. Rev.* **2015**, DOI: 10.1039/C4CS00171K.
[5] G. X. Bai, M. K. Tsang, J. H. Hao, *Adv. Opt. Mater.* **2014**, DOI: 10.1002/adom.201400375.
[6] J. Li, J. H. Zhang, Z. D. Hao, X. Zhang, J. H. Zhao, Y. S. Luo, *Appl. Phys. Lett.* **2012**, *101*, 121905.
[7] E. De la Rosa, P. Salas, H. Desirena, C. Angeles, R. A. Rodríguez, *Appl. Phys. Lett.* **2005**, *87*, 241912.
[8] Z. D. Hao, J. H. Zhang, X. Zhang, X. J. Wang, *Opt. Mater.* **2011**, *33*, 355 – 358.
[9] Y. Yu, Y. D. Zheng, F. Qin, L. X. Liu, C. B. Zheng, G. Y. Chen, Z. G. Zhang, W. W. Cao, *Opt. Commun.* **2011**, *284*, 1053 – 1056.
[10] J. Li, J. H. Zhang, Z. D. Hao, X. Zhang, J. H. Zhao, Y. S. Luo, *ChemPhysChem* **2013**, *14*, 4114 – 4120.
[11] M. M. Broer, D. L. Huber, W. M. Yen, W. K. Zwicker, *Phys. Rev. Lett.* **1982**, *49*, 394 – 397.
[12] Y. Zhang, J. H. Hao, *J. Mater. Chem. C* **2013**, *1*, 5607 – 5618.
[13] M. Stalder, M. Bass, *J. Opt. Soc. Am. B* **1991**, *8*, 177 – 183.
[14] S. Guy, *Phys. Rev. B* **2006**, *73*, 144101.
[15] R. P. Leavitt, J. B. Gruber, N. C. Chang, C. A. Morrison, *J. Chem. Phys.* **1982**, *76*, 4775 – 4788.

Received: January 4, 2015
Published online on February 26, 2015